

## Functionalization of Electrospun Nanofibers of Natural Cotton Cellulose by Cerium Dioxide Nanoparticles for Ultraviolet Protection

Chaorong Li, Shunxin Shu, Rui Chen, Benyong Chen, Wenjun Dong

Department of Physics and Key Laboratory of ATMMT Ministry of Education, Zhejiang Sci-Tech University, Hangzhou 310018, People's Republic of China  
Correspondence to: C.-R. Li (E-mail: crli@zstu.edu.cn)

**ABSTRACT:** Nanofibers of natural cotton cellulose with a degree of polymerization above 10,000 were prepared by electrospinning; they were then functionalized with a rare-earth nano-oxide material of cerium dioxide ( $\text{CeO}_2$ ) by means of the hydrothermal method to obtain the designated properties. The morphology, structure, and properties of the as-obtained nanocomposite fibers were characterized by scanning electron microscopy, transmission electron microscopy, energy-dispersive spectroscopy, X-ray diffraction, Fourier transform infrared spectroscopy, and ultraviolet (UV)–visible spectrophotometry. The results show that hydrothermally grown  $\text{CeO}_2$  nanoparticles exhibited a polycrystalline cubic fluorite structure and could be dispersed uniformly on the surface of the cellulose nanofiber. The strong interface and electrostatic interactions between the nanoparticles and nanofibers effectively prevented nanoparticle fall-off. The modified natural cotton cellulose nanofibers showed excellent protection against UV radiation because of the function of the  $\text{CeO}_2$  particles. Such cellulose nanocomposite materials could have potential applications in UV protection for data-storage or memory devices. © 2013 Wiley Periodicals, Inc. *J. Appl. Polym. Sci.* 130: 1524–1529, 2013

**KEYWORDS:** composites; electrospinning; fibers; functionalization of polymers; nanostructured polymers

Received 3 January 2013; accepted 4 March 2013; Published online 30 April 2013

**DOI:** 10.1002/app.39264

### INTRODUCTION

Cellulose is considered a prime unlimited alternative, sustainable, and renewable biopolymer resource; it holds very attractive properties, including biocompatibility, biodegradability, and thermal and chemical stability.<sup>1</sup> The content of cellulose in cotton fiber is far higher than in those in wood, flax, straw, and other plants. Cotton is the most pure natural cellulose source. The traditional application for cotton fiber is in the cotton fabric industry in its primitive state. Therefore, it is important to functionalize cotton fibers and expand their application areas. Previous researchers' efforts have been put forth to modify conventional cotton fabrics via inorganic oxide coatings, and this has resulted in some unique properties. Becheri et al.<sup>2</sup> made composites of nanosized ZnO particles with cellulose fibers to create UV shielding with the hydrothermal method. He et al.<sup>3</sup> successfully developed a facile method for the *in situ* synthesis of  $\text{MnO}_2$  nanosheets on porous cellulose fibers and obtained functional nanocomposites for a higher efficiency catalytic formaldehyde compared to that of  $\text{MnO}_2$  powder. Wu et al.<sup>4</sup> prepared self-cleaning and bactericidal cotton fabrics by depositing and grafting  $\text{TiO}_2$  nanoparticles via an aqueous sol process at low temperature. Generally, these functions can be added to textiles via surface modification and without detrimental effects

on the mechanical properties of textile fabrics. Therefore, the incorporation of various functional nanomaterials into cotton fabrics is one of the most effective ways of improving the properties of cotton fabrics. However, the main problem is the poor interfacial bonding force for microscale cotton fibers and functional nanometer material.

Natural cellulose fibers and cotton fabrics have a porous structure and are composed of microfibrils 10–30  $\mu\text{m}$  in width that are connected with each other three-dimensionally.<sup>5</sup> Compared with microfibrils, nanofibers reveal many amazing characteristics, including a high surface volume value and a small fiber diameter.<sup>6–8</sup> This makes them to a competing candidate for many important applications in tissue scaffolds, protective clothing, and optical electronics.<sup>9–11</sup> Being an efficient technique for the fabrication of nanofibers, electrospinning has received a surprising attention in recent years. Natural cotton cellulose nanofibers obtained by means of the electrospinning technique are more conductive than cotton fabrics to functionalization because of the large number of favorable coordination active sites provided by the nanofibers. However, rare reports have touched on the cotton nanofibers' unique structure, large specific surface area, and potential usage in templates. The functionalization of electrospun natural cotton cellulose fibers with an inorganic oxide

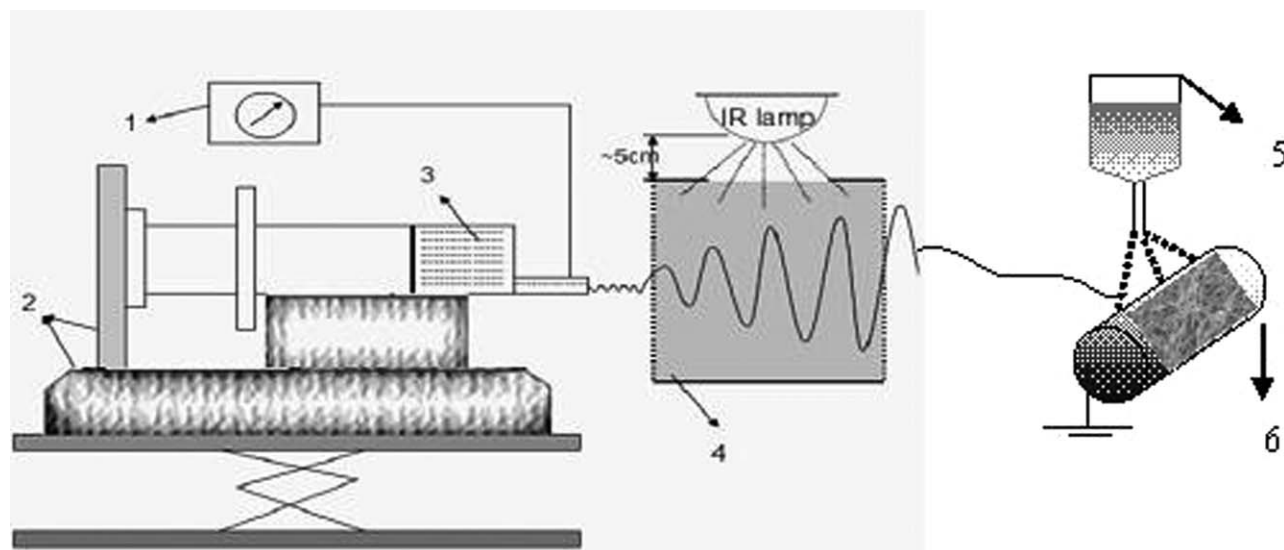


**Figure 1.** Setup used for the electrospinning of the cellulose nanofibers: (1) high voltage, (2) pump, (3) solution, (4) heater and heating range, (5) water tank, and (6) drum.

coating has rarely been studied so far. The main barrier is the low solubility and bad spinnability of natural cotton cellulose. In recent years, our research group developed a highly energy-efficient, one-step method to obtain ultrafine cellulose nanofibers from the natural cotton cellulose with a degree of polymerization (DP) above 10,000. The incorporation of inorganic nanoparticles into a cellulose nanofiber substrate can significantly modify the properties of the nanofibers. The obtained nanocomposite nanofibers might exhibit improved thermal, mechanical, or optical properties, which are determined by the composited inorganic materials.

In recent years, increasing concern over excessive terrestrial UV radiation as a kind of environmental pollution has pushed the occurrence of extensive studies of UV-blocking textiles.<sup>12–14</sup> The formation of self-cleaning and UV coating surfaces, particularly those based on dip-pad-cure and dip-coating processes and sol-gel and hydrothermal methods have been studied extensively by many researchers.<sup>15–17</sup> Some inorganic oxides, such as ZnO, TiO<sub>2</sub>, and cerium dioxide (CeO<sub>2</sub>), have been widely used in the field of UV blocking; this has included applications on the surface of textile fabrics to provide UV protection. Because of its optical, magnetic, and electronic properties, CeO<sub>2</sub> has been widely used in various applications, including catalysis, optical materials, abrasives, and particularly UV absorbents; this makes it highly promising as a material for a wide range of UV blockers.<sup>18–20</sup>

In this study, we developed a facile and effective method for the *in situ* synthesis of CeO<sub>2</sub> nanoparticles on electrospun cotton nanofibers. The nanofibers act as a unique nanoreactor and template and as a support. The UV absorption performance of the obtained nanocomposite fibers were investigated. The dependence of the efficiency for UV protection on a number of parameters, including the particles size and crystallization properties, was also systematically investigated. The research results

not only give full play to the advantages of cotton nanofibers but also expand its application areas.

## EXPERIMENTAL

### Materials

Cotton cellulose with a DP of 12,000 was provided by Zhejiang Academy of Agricultural Sciences. The chemicals, including methanol [CH<sub>3</sub>OH; ≥99.5%, analytical reagent (AR)], anhydrous ethanol (C<sub>2</sub>H<sub>5</sub>OH, ≥99.7%, AR) were purchased from Hangzhou Gaojing Chemical Reagent Co., Ltd. *N,N*-Dimethylacetamide (DMAc; ≥99.5%, AR), hexamethylene tetramine (HMT; ≥99.0%, AR), and cerium nitrate hexahydrate [Ce(N-O<sub>3</sub>)<sub>3</sub>·6H<sub>2</sub>O, ≥99.5%, AR], were supplied by Tianjin YongDa Chemical Reagent Development Center. These resources and chemicals were used without further purification. Lithium chloride (LiCl; ≥99.5%, AR) from Aladdin Chemistry Co., Ltd., was preprocessed to remove water.

### Preparation of the Nanofibers of Natural Cotton Cellulose via Electrospinning

Before the dissolution of the natural cotton cellulose, an activation treatment was performed to weaken the polymer chains into a relaxed conformation. The pretreatment process, which followed that of Li et al.,<sup>21</sup> included the following processes: (1) the immersion of natural cellulose in water for 1 night and the subsequent removal of the water, (2) the washing of the swollen cellulose with methanol twice consecutively, and (3) two exchanges with DMAc. All of these immersions and exchanges were conducted at room temperature. Finally, the cellulose was filtered *in vacuo* and dried for the next dissolution procedure. The electrospinning solution was prepared by the dissolution of 1.15% w/v activated cellulose into the LiCl/DMAc solvent mixture, in which LiCl was set at 8.0% w/v. In the electrospinning process, the prepared solution was electrospun by a self-made apparatus on the basis of the characteristics of a cellulose

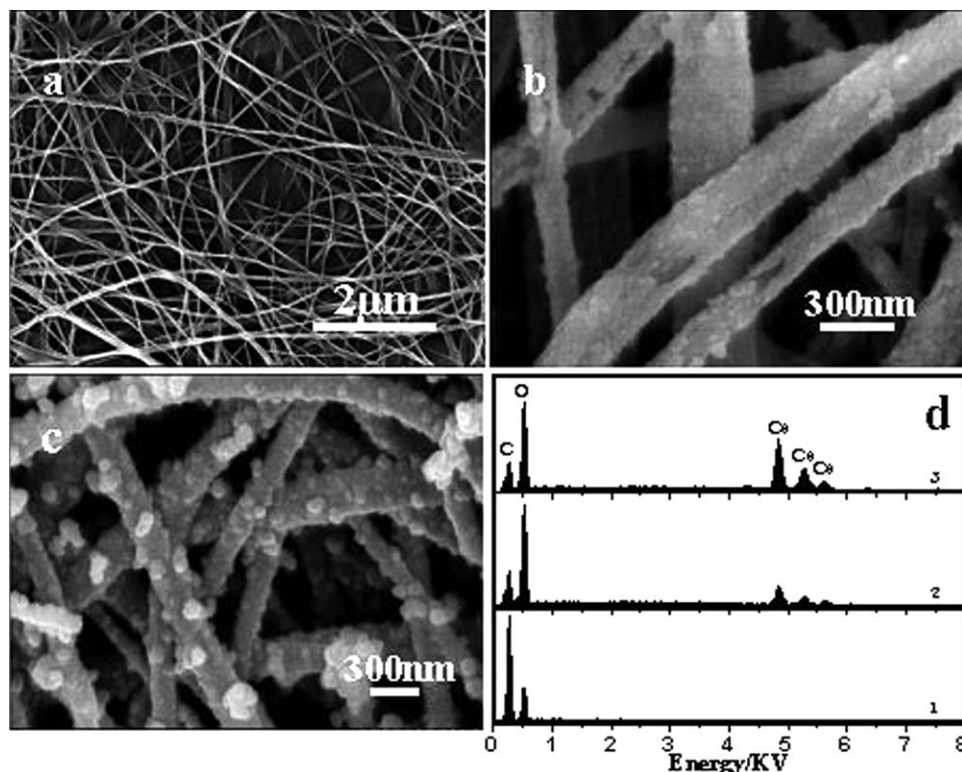


**Figure 2.** SEM images of the (a) electrospun cotton cellulose nanofibers, (b) nanofibers coated with  $\text{CeO}_2$  nanoparticles by a hydrothermal reaction of 3 h, and (c) nanofibers coated with  $\text{CeO}_2$  nanoparticles by a hydrothermal reaction of 6 h and (d) EDS spectrum of the (d1) electrospun nanofibers and (d2,d3) nanofibers coated with  $\text{CeO}_2$  nanoparticles.

spinning solution, as shown in Figure 1. The precursor solution was electrospun at a 21-kV voltage, a 12-cm working distance, and 0.8 mL/h flow rate. The as-collected nanofibers were immersed in deionized water for 1 night to adequately remove residual solvents and were then dried at room temperature prior to further treatment.

#### Fabrication of the $\text{CeO}_2$ /Cotton Cellulose Nanocomposites

In a typical synthesis procedure, 1.25 mmol of  $\text{Ce}(\text{NO}_3)_3 \cdot 6\text{H}_2\text{O}$  was dissolved in 25 mL of deionized water to form a transparent solution and then 3.75 mmol of HMT was added. The solution was stirred vigorously for 30 min, and the as-obtained nanofiber mats were immersed in the transparent solution and then poured into a Teflon-lined stainless steel autoclave. After being sealed, the vessel was placed into a thermostated oven at a temperature of 120°C and kept there for 3 or 6 h. After they cooled down to room temperature naturally, the nanofiber mats were washed with deionized water and anhydrous alcohol three times to remove other ions and were then dried at room temperature.

#### Instruments and Characterization

The surface morphology of the nanofibers were studied by field-emission scanning electron microscopy (FESEM; Hitachi S-4800) and transmission electron microscopy (TEM; JEM 2100, 200 kV). The structural properties of the nanofibers were characterized by X-ray diffraction (XRD; Bruker AXS D8-Discover) with  $\text{Cu K}\alpha$  radiation ( $\lambda = 0.15405$  nm at 40 kV and 40

mA). Fourier transform infrared (FTIR) spectra were obtained on an FTIR spectroscope (Nicolet Avatar 370). An ultraviolet–visible (UV–vis) absorption spectrophotometer (U-3900 Hitachi) was used to investigate the UV performance properties of the nanocomposites.

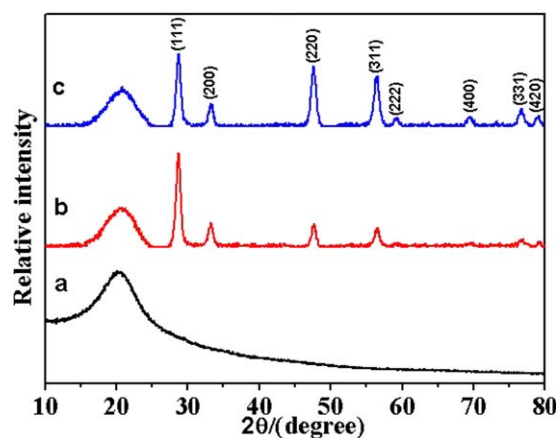


**Figure 3.** XRD patterns of the as-fabricated samples: (a) natural cotton cellulose nanofibers, (b) nanofibers coated with  $\text{CeO}_2$  nanoparticles by a hydrothermal reaction of 3 h, and (c) nanofibers coated with  $\text{CeO}_2$  nanoparticles by a hydrothermal reaction of 6 h. [Color figure can be viewed in the online issue, which is available at [wileyonlinelibrary.com](http://wileyonlinelibrary.com).]

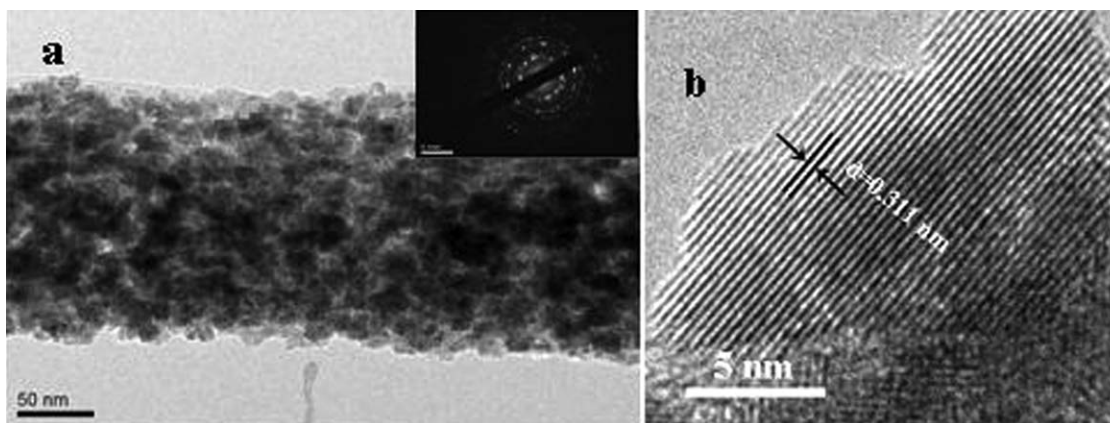


**Figure 4.** (a) TEM and (b) HRTEM images of cotton cellulose/CeO<sub>2</sub> nanocomposites formed by a hydrothermal reaction of 6 h. [Inset part is the selected area electron diffraction from CeO<sub>2</sub> nanoparticles].

## RESULTS AND DISCUSSION

Scanning electron microscopy (SEM) images were used to observe the morphologies of the cotton nanofiber and treated cotton nanofibers by a hydrothermal reaction. We observed that the as-spun nanofibers [Figure 2(a)], with diameters from 100 to 200 nm, showed very smooth surfaces. There were rarely adhesions or aggregations at the intersection of the electrospun fibers. In the case of the 3-h hydrothermal reaction, the small CeO<sub>2</sub> nanoparticles dispersed greatly on the surface of the natural cellulose nanofibers, and the size of the CeO<sub>2</sub> nanoparticles was in the range 40–60 nm, as displayed in Figure 2(b). With the elongation of the reaction time to 6 h, the CeO<sub>2</sub> nanoparticles grew up to about 100–120 nm, as shown in Figure 2(c). To determine the chemical elements of the cotton nanofibers and cotton nanofibers treated by the hydrothermal reaction, the samples were characterized by energy-dispersive spectroscopy (EDS). Figure 2(d-1) gives a typical EDS spectrum recorded for the cotton nanofibers. The results confirm the presence of the C and O elements without other elements in the cotton nanofibers. This was attributed to the absence of residual solvents in the nanofibers. EDS spectra [Figure 2(d-1,d-3)] were recorded for the cotton cellulose/CeO<sub>2</sub> nanocomposites obtained under hydrothermal treatment for 3 and 6 h, respectively. The Ce element could be detected from the EDS spectrum. With the extension of the reaction time, the peak of the Ce element increased obviously, and this confirmed that more and more CeO<sub>2</sub> particles were effectively coated onto the cotton nanofiber surface.

XRD analysis was used to examine the crystal structure of the as-prepared samples, as shown in Figure 3. Figure 3(a) shows the broad diffraction peaks of the natural cotton cellulose nanofibers at 15–25°, which were ascribed to the amorphous cellulose structure. After hydrothermal treatment at 120°C for 3 h [(Figure 3(b)), compared to curve a for the natural cotton cellulose nanofibers, new peaks were observed in curve b, which were attributed to the diffraction peaks of the (111), (220), (200), (311), (222), (400), (331), and (420) planes of CeO<sub>2</sub> with the cubic fluorite structure reported by the International Center for Diffraction Data (JCPDS data number 43-1002 card). At the same time, the diffraction peaks of the cubic fluorite CeO<sub>2</sub> were

enhancement with the extension of hydrothermal time; this indicated that the crystallinity of the sample improved accordingly. Additionally, no impure peaks were detected from these figures; this clearly illustrated the high purity of all of the as-prepared samples. When the XRD analyses were combined with the FESEM results, we concluded that the method adopted in this study was beneficial for acquiring the cellulose/CeO<sub>2</sub> nanocomposite structure, which was composed of the cubic fluorite structure CeO<sub>2</sub> and cellulose nanofibers.

Figure 4 shows the representative TEM and high-resolution transmission electron microscopy (HRTEM) micrographs of the cellulose/CeO<sub>2</sub> nanocomposites fabricated under hydrothermal treatment for 6 h. As shown in Figure 4(a), the TEM image shows that a large quantity of uniform distribution CeO<sub>2</sub> nanoparticles were attached to the surface of the natural cotton cellulose nanofiber substrate, and the inset shows a selected area of the electron diffraction pattern. The diffraction pattern of the CeO<sub>2</sub> nanoparticles exhibited a polycrystalline structure. Meanwhile, an HRTEM image of the cotton cellulose/CeO<sub>2</sub> nanocomposites is shown in Figure 4(b), where the clear lattice fringe at 0.311 nm corresponds to the (111) plane of the cubic fluorite phase of the CeO<sub>2</sub> nanoparticles.

To evaluate the interactions between the natural cotton cellulose nanofibers and the CeO<sub>2</sub> nanoparticles in the hybrid fibers, FTIR was applied, as shown in Figure 5. As shown in Figure 5(a), the spectrum of the cotton cellulose nanofiber exhibited an O–H stretching absorption around 3440 cm<sup>-1</sup>, a C–H stretching absorption around 2985 cm<sup>-1</sup>, a C–O–C stretching absorption around 1164 cm<sup>-1</sup>, a C–OH stretching absorption around 1068 cm<sup>-1</sup>, and a C–O stretching absorption around 1026 cm<sup>-1</sup>. These absorptions were consistent with those of a typical cellulose backbone. The peaks for the cotton cellulose/CeO<sub>2</sub> nanocomposite fibers [(Figure 5(b)) were weakened in comparison to the peaks for the cotton cellulose nanofibers because the CeO<sub>2</sub> nanoparticles grew on the surface of the cotton cellulose nanofibers. A characteristic IR band at 1643 cm<sup>-1</sup>, corresponding to the O=C vibrations of the cotton cellulose, shifted greatly to lower wave numbers (from 1643 to 1568 cm<sup>-1</sup>); this indicated that a strong interaction occurred at the

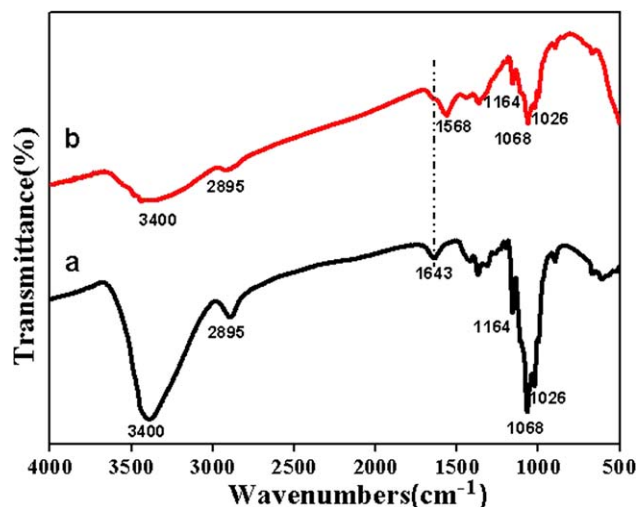


**Figure 5.** FTIR spectra of (a) natural cotton cellulose nanofibers and (b) nanofibers coated with  $\text{CeO}_2$  nanoparticles by a hydrothermal reaction of 6 h. [Color figure can be viewed in the online issue, which is available at [wileyonlinelibrary.com](http://wileyonlinelibrary.com).]

interface of the cotton cellulose nanofibers and  $\text{CeO}_2$  nanoparticles. Therefore, although the  $\text{CeO}_2$  coating was a deposit on the surface of the cotton cellulose nanofibers, the contact could have been well developed because of the strong interfacial and electrostatic interactions between the carboxylic groups or hydroxyl groups and cerium atoms. A similar phenomenon was observed for the C—H stretching vibrations ( $2895\text{ cm}^{-1}$ ). Because of the coverage by thin layer of  $\text{CeO}_2$ , this C—H in-plane stretching was blocked as result of steric hindrance. We observed that the characteristic absorption bands in the whole range were basically unchanged; this indicated that the chemical structure of the cotton cellulose was not altered under hydrothermal conditions.

On the basis of the experimental results, the overall possible chemical reaction process for the cotton cellulose/ $\text{CeO}_2$  nanocomposite structure during hydrothermal treatment is illustrated in Figure 6. In the first stage, the  $\text{Ce}^{3+}$  of  $\text{Ce}(\text{NO}_3)_3 \cdot 6\text{H}_2\text{O}$  in a water solution reacted with the surface hydroxyl groups of the cellulose nanofibers via an electrostatic interaction. HMT is a nontoxic, water-soluble, and nonionic tetradentate cyclic tertiary amine, which released hydroxyl ions at an elevated temperature. Subsequently, under solvothermal conditions,  $\text{Ce}(\text{OH})_3$  precursor seeds were formed by a chemical reaction. As a result,  $\text{Ce}(\text{OH})_3$  precursor seeds nucleated through the heterogeneous nucleation process on active growth sites provided by the natural cotton cellulose nanofibers templates. Finally, the  $\text{CeO}_2$  nanoparticles took shape from the  $\text{Ce}(\text{OH})_3$  precursors by oxidation in a solution of dissolved oxygen. In principle, the surface energies of large particles were lower than those of smaller ones. Therefore, the small  $\text{CeO}_2$  nanoparticles were inclined to grow larger as the reaction continued via the so-called Ostwald ripening process.

The UV-shielding ability of the cotton cellulose/ $\text{CeO}_2$  nanocomposites was evaluated by UV-vis absorption spectroscopy, as shown in Figure 7. From Figure 7, we observed a remarkable absorption in the UV region, and the absorption increased dramatically at wavelengths above 350 nm; this indicated that the natural cotton cellulose nanofiber modified with  $\text{CeO}_2$  nanoparticles could offer better protection from UV radiation than the natural cotton cellulose nanofibers. It was obvious that along with the increase of  $\text{CeO}_2$  nanoparticles, the crystallization properties and UV absorption performance increased significantly. This was due to the following two possible reasons:

1.  $\text{CeO}_2$  caused good UV absorption as a result of its  $4f^1$  electronic structure and rich electronic warp level. It is very sensitive to light absorption and shows absorption bands mostly in the UV area.

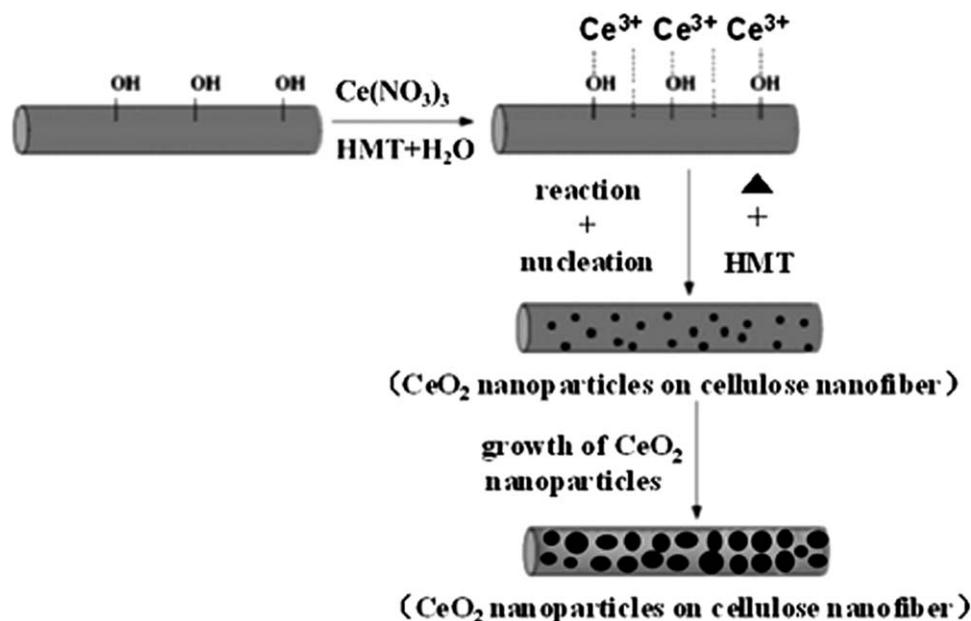


**Figure 6.** Scheme of the formation process of  $\text{CeO}_2$  nanoparticles on the nanofiber substrate by the hydrothermal reaction.

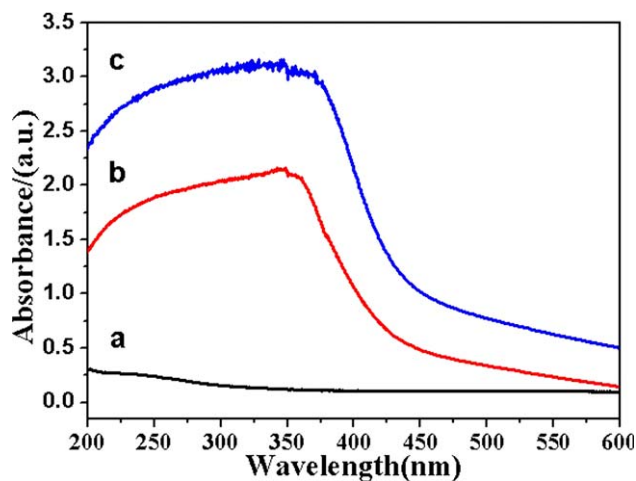


**Figure 7.** UV-vis absorption spectra of (a) natural cotton cellulose nanofibers, (b) CeO<sub>2</sub>-nanoparticle-coated nanofibers formed by a hydrothermal reaction of 3 h, and (c) CeO<sub>2</sub>-nanoparticle-coated nanofibers formed by a hydrothermal reaction of 6 h. [Color figure can be viewed in the online issue, which is available at [wileyonlinelibrary.com](http://wileyonlinelibrary.com).]

- The formation of a CeO<sub>2</sub> nanoparticle uniform distribution on the natural cotton cellulose nanofiber surface imparted a very efficient UV scattering because of the large refractive index of the CeO<sub>2</sub> nanoparticles.

## CONCLUSIONS

In summary, with electrospinning technology, a more energy-efficient one-step method for obtaining ultrafine cellulose fibers from natural cotton lines, whose DP was above 10,000, was developed. The cellulose nanofibers treated with the hydrothermal incorporation of CeO<sub>2</sub> nanoparticles into the nanofiber substrate surface showed excellent UV-shielding properties compared to the natural cotton cellulose nanofibers. CeO<sub>2</sub> nanoparticles were attached to the surface of the nanofiber substrate because of strong interfacial and electrostatic interactions between the active groups of the nanofiber surface and the CeO<sub>2</sub> nanoparticles. In addition, the fabrication process of such functional nanofibers could easily be applied without expensive raw materials and complex methods. This functional nanofiber will have potential applications in various areas, such as the medical, military, biological, and optoelectronic industrial fields, in the future.

## ACKNOWLEDGMENTS

This work was supported by the Natural Science Foundation of China (contract grant numbers 51172209 and 91122022).

## REFERENCES

- Seifert, M.; Hesse, S.; Kabrelian, V.; Klemm, D. J. *Polym. Sci. Part A: Polym. Chem.* **2004**, *42*, 463.
- Becheri, A.; Dürr, M.; Nostro, P. L.; Baglioni, P. J. *Nanopart. Res.* **2008**, *10*, 679.
- Zhou, L.; He, J. H.; Zhang, J.; He, Z. C.; Hu, Y. C.; Zhang, C. B.; He, H. J. *Phys. Chem. C* **2011**, *115*, 16873.
- Wu, D. Y.; Long, M. C.; Zhou, J. Y.; Cai, W. M.; Zhu, X. H.; Chen, C.; Wu, Y. H. *Surf. Coat. Technol.* **2009**, *203*, 3728.
- He, J. H.; Kunitake, T.; Nakao, A. *Chem. Mater.* **2003**, *15*, 4401.
- Subbiah, T.; Bhat, G. S.; Tock, R. W.; Parameswaran, S.; Ramkumar, S. S. *J. Appl. Polym. Sci.* **2005**, *96*, 557.
- Frenot, A.; Chronakis, I. S. *Curr. Opin. Colloid Interface Sci.* **2003**, *8*, 64.
- Zheng, M. H.; Zhang, Y. Z.; Kotaki, M.; Ramakrishna, S. *Compos. Sci. Technol.* **2003**, *63*, 2223.
- Li, W. L.; Laurencin, C. T.; Catterson, E. J.; Tuan, R. S.; Ko, F. K. *J. Biomed. Mater. Res.* **2002**, *60*, 613.
- Shin, Y. M.; Hohman, M. M.; Brenner, M. P.; Rutledge, G. C. *Polymer* **2001**, *42*, 9955.
- Huang, Z. M.; Zhang, Y. Z.; Kotaki, M.; Ramakrishna, S. *Compos. Sci. Technol.* **2003**, *63*, 2223.
- Lu, H.; Fei, B.; Xin, J. H.; Wang, R.; Li, L. J. *Colloid. Interface. Sci.* **2006**, *300*, 111.
- Tragoonwichian, S.; O'Rear, E. A.; Yanumet, N. J. *Appl. Polym. Sci.* **2008**, *108*, 4004.
- Onar, N.; Ebeoglugil, M. F.; Kayatekin, I.; Celik, E. J. *Appl. Polym.* **2007**, *106*, 514.
- Wang, R. H.; Xin, J. H.; Tao, X. M. *Inorg. Chem.* **2005**, *44*, 3926.
- Wu, D. Y.; Long, M. C.; Zhou, J. Y.; Cai, W. M.; Zhu, X. H.; Chen, C.; Wu, Y. H. *Surf. Coat. Technol.* **2009**, *203*, 3728.
- Wu, Z. B.; Gu, Z. L.; Zhao, W. R.; Wang, H. Q. *Chin. Sci. Bull.* **2007**, *52*, 3061.
- Tao, Y.; Gong, F. H.; Wang, H.; Wu, H. P.; Tao, G. L. *Mater. Chem. Phys.* **2008**, *112*, 973.
- Ji, P.; Zhang, J.; Chen, F.; Anpo, M. *Appl. Catal. B.* **2009**, *85*, 148.
- Yu, S. H.; Cölfen, H.; Fischer, A. *Colloid. Surf. A* **2004**, *243*, 49.
- Li, C. R.; Chen, R.; Zhang, X. Q.; Shu, S. X.; Xiong, J.; Zheng, Y. Y.; Dong, W. J. *Fiber Polym.* **2011**, *12*, 345.